

# Modified Bismuth Nanoparticles: A New Targeted Nanoprobe for Computed Tomography Imaging of Cancer

Milad Mohammadi, M.Sc.<sup>1</sup>, Sara Khademi, Ph.D.<sup>2</sup>, Yazdan Choghazardi, Ph.D.<sup>3</sup>, Rasoul Irajirad, Ph.D.<sup>4</sup>,  
 Mohammad Keshtkar, Ph.D.<sup>5\*</sup>, Alireza Montazerabadi, Ph.D.<sup>1\*</sup>

1. Medical Physics Research Center, Mashhad University of Medical Sciences, Mashhad, Iran

2. Department of Radiology Technology, School of Paramedical Sciences, Mashhad University of Medical Sciences, Mashhad, Iran

3. Department of Medical Physics, Faculty of Medicine, Isfahan University of Medical Sciences, Isfahan, Iran

4. Department of Medical Physics, School of Medicine, Iran University of Medical Sciences, Tehran, Iran

5. Medical Physics and Radiology Department, Faculty of Medicine, Gonabad University of Medical Sciences, Gonabad, Iran

\*Corresponding Addresses: P.O.Box: 9691983879, Medical Physics and Radiology Department, Faculty of Medicine, Gonabad University of Medical Sciences, Gonabad, Iran

P.O.Box: 9177948564, Medical Physics Research Center, Mashhad University of Medical Sciences, Mashhad, Iran

Emails: keshtkar.dmohammad@yahoo.com, montazerabadi@mums.ac.i

Received: 14/November/2021, Accepted: 08/March/2022

## Abstract

**Objective:** Recently, development of multifunctional contrast agent for effective targeted molecular computed tomography (CT) imaging of cancer cells stays a major problem. In this study, we explain the ability of Triptorelin peptide-targeted multifunctional bismuth nanoparticles (Bi<sub>2</sub>S<sub>3</sub>@ BSA-Triptorelin NPs) for molecular CT imaging.

**Materials and Methods:** In this experimental study, the formed nanocomplex of Bi<sub>2</sub>S<sub>3</sub>@ BSA-Triptorelin NPs was characterized using different methods. The MTT cytotoxicity test was performed to determine the appropriate concentration of nanoparticles in the MCF-7 cells. The X-ray attenuation intensity and Contrast to Noise Ratio (CNR) of targeted and non-targeted nanoparticles were measured at the concentrations of 25, 50, and 75 µg/ml and X-ray tube voltages of 90, 120 and 140 kVp.

**Results:** We showed that the formed Bi<sub>2</sub>S<sub>3</sub>@ BSA-Triptorelin NPs with a Bi core size of approximately ~8.6 nm are nontoxic in a given concentration (0-200 µg/ml). At 90, 120, and 140 tube potentials (kVp), the X-ray attenuation of targeted cells were 1.35, 1.36, and 1.33-times, respectively, more than non-targeted MCF-7 cells at the concentration of 75 µg/ml. The CNR values at 90, 120, and 140 kVp tube potentials were 171.5, 153.8 and 146.3 c/ε, respectively.

**Conclusion:** These findings propose that the diagnostic nanocomplex of Bi<sub>2</sub>S<sub>3</sub>@ BSA-Triptorelin NPs can be applied as a good contrast medium for molecular CT techniques.

**Keywords:** CT Contrast Agents, Molecular Imaging, Targeted Imaging, Triptorelin

Cell Journal (Yakhteh), Vol 24, No 9, September 2022, Pages: 515-521

**Citation:** Mohammadi M, Khademi S, Choghazardi Y, Irajirad R, Keshtkar M, Montazerabadi A. Modified bismuth nanoparticles: a new targeted nanoprobe for computed tomography imaging of cancer. Cell J. 2022; 24(9): 515-521. doi: 10.22074/cellj.2022.8348.

This open-access article has been published under the terms of the Creative Commons Attribution Non-Commercial 3.0 (CC BY-NC 3.0).

## Introduction

Molecular imaging involves the visualization, diagnosis, and quantification of physiological and pathological processes of the body at the cellular and/or molecular level. The biochemical markers and/or other markers molecules provide this aim (1). Either alone or in the combination with imaging agents can image the tissue state. Today, a computed tomography (CT) imaging, a relatively inexpensive, high-resolution method, is used in 75% of all of clinical diagnostic imaging. CT imaging shows higher resolution of spatial and temporal (2), but is less sensitive than other clinical imaging modalities (3). To date small iodine-based molecular compounds used, such as Visipaque, show various disadvantages, including toxicity of renal, short half-lives, and absence of specificity (4, 5). To improve the sensitivity of the images, the new contrast media should include the following properties: surface chemical modification, high atomic number, sufficient concentration, size control, biocompatible and be targeted (4, 6).

Bismuth (atomic number of 83 and k-edge=90.5 KeV)

may be a potential candidate to be a contrast enhancer in CT imaging (7). Especially compared to conventional iodine contrast agents, Bi<sub>2</sub>S<sub>3</sub> offers several favorable features, including cost-effective, long half-lives, and capability to embrace functional surface changes (5, 8). Molecular imaging largely depends on the development of specificity and sensitivity of imaging agents (9). Targeting agents such as small molecules, peptides, antibodies, and aptamers (10) are used to label imaging agents as a ligand detector (11). Compared to small molecules, peptides have many advantages, such as good selectivity and specificity, and easy formulation that do not require any binding properties alteration. In addition, peptides are more stable than antibodies at the room temperature and have less immunogenicity than antibodies (10). The gonadotropin-releasing hormone (GnRH), as well called as hypothalamic luteinizing hormone-releasing hormone (LHRH) been proposed as targets for targeted cancer treatment (12). The LHRH is a decapeptide hormone with the primary sequence pGlu-His-Trp-Ser-Tyr-Gly-Leu-Arg-Pro-Gly-NH<sub>2</sub> that secretes from the hypothalamus.

LHRH can bind specifically to Luteinizing Hormone Releasing Hormone Receptor (LHRH-R) at the surface of gonadotropin cells in the pituitary gland and stimulate the synthesis and release of luteinizing hormone (LH) and follicle-stimulating hormone (FSH) (13).

Some tumors express LHRH receptors on their surfaces, like breast, ovary, prostate (14, 15). Therefore, the presence of specific sites for the binding of LHRHs on the membrane of cancer cells provides the conditions for the binding of LHRH as well as its analogues, which also have a high affinity for these cells (16). On the other hand, due to the limited expression of these receptors in normal tissues, it can be used for targeted drug delivery, such as an imaging agent or therapy for LHRH-R<sup>+</sup> tumors (containing hormone receptors). In some cases, LHRH antibodies or peptides that bind to LHRH-R are used to deliver contrast agents in various imaging modalities such as ultrasound, MRI, PET, and SPECT to the expressing LHRH-R cells (17). Triptorelin is a deca peptide with the pGlu-His-Trp-Ser-Tyr-D-Trp-Leu-Arg-Pro-Gly-NH<sub>2</sub> sequence that has a molecular weight of 1311.4 g/mol (13, 18). Receptors are detected by these hormonal peptides, so they can be internalized after binding to their ligands (19). In this study, we synthesized and evaluated the cytocompatibility of the multifunctional Triptorelin peptide conjugated bismuth nanoparticles (Bi2S3@ BSA-Triptorelin NPs). Furthermore, the synthesis of Bi2S3 @ BSA with and without targeting molecule (Triptorelin) was measured for molecular CT technique at various concentrations NPs, and X-ray tube voltages.

## Material and Method

This study was approved by the Ethical Research Committee of Mashhad University of Medical Sciences (IR.MUMS.MEDICAL.REC.1398.557).

### Preparation of Bi2S3 @ BSA nanoparticles

Briefly, under stirring, aqueous Bi (NO<sub>3</sub>)<sub>3</sub> (248592, Sigma Aldrich, USA) (2.8 mL in 3 M HNO<sub>3</sub> solution (438073, Sigma Aldrich, USA), 25 mM, 25°C) was added into the BSA solution (40 mL, 66 mg/mL) (810533, Sigma Aldrich, USA) at 25°C temperature. Adding bismuth solution should not take more than 2 minutes. Then, add 6 ml of sodium hydroxide solution (5 M) (S8045, Sigma Aldrich, USA) at once to the above solution. Eventually the color of the solution starts to modify from yellow to brown, and after that to dark black for 10 minutes. The mixture was set aside for another 12 hours to complete the reaction without rotation. All synthesis steps were performed at room temperature. Finally, the product was centrifuged at 12,000 rpm for 15 minutes, reaching a volume of 2.5 cc, and finally dialyzed for 48 hours (20).

### Binding of Triptorelin peptide to nanoparticles

1 ml of the above final product was magnetically stirred to a pH of 6.5, then 0.5 mg of peptide was added, and finally 0.15 mg of N-(3-dimethylaminopropyl)-N-ethylcarbodiimide hydrochloride (EDC) (8.51007, Sigma-Aldrich, USA) and 0.09 mg of the N-Hydroxysuccinimide

(NHS) (130672, Sigma-Aldrich, USA) was added. The reaction was stirred for 1 hour at room temperature. The final product was dialyzed for 24 hours in refrigerator to obtain Bi2S3@BSA-Triptorelin NPs.

### Characterization techniques

Morphology and size distribution of nanoparticles were evaluated using transmission electron microscope (TEM) (Gatan model 791, Philips CM 12, Poland) and image J, respectively. X-ray Diffraction (XRD) patterns of dried nanoparticle powders were analyzed through the GNR EXPLORER (XRD) X-ray diffraction gauge with a wavelength of 1.54 Å K<sub>α</sub> lines. Fourier Transform Infrared (FTIR) spectra were evaluated using an infrared spectrometer Red (AVATAR 370, Thermo Nicolet AVATAR 370 FTIR, USA). The surface charge of nanoparticles and the hydrodynamic size of nanoparticles were measured by a device (SZ100, HORIBA, Japan). The contents of bismuth in the samples were measured using Inductively Coupled Plasma - Optical Emission Spectrometry (ICP-OES) (VISTA-MPX, Varian Inc., USA).

### Stability of Bi2S3@BSA-Triptorelin NPs

The stability of Bi2S3@BSA-Triptorelin NPs was evaluated using DLS analysis. 100 μl of Bi2S3@ BSA-Triptorelin NPs was added to 500 μl of 10% FBS (16000044, GIBCO, USA) culture medium. After 24 hours, the hydrodynamic size of nanoparticles was assessed from the obtained solution. The result was compared with the hydrodynamic size obtained from the DLS test of Bi2S3@BSA-Triptorelin nanoparticles.

### X-ray attenuation measurements of Bi2S3@BSA-Triptorelin NPs versus Visipaque

The X-ray attenuation intensity of Bi2S3 @ BSA Triptorelin NPs was compared with CT contrast agent based on iodine Visipaque (320 mg/ml), (544031, GE Healthcare, Ireland). Different concentrations (500-3000 μg/ml) of the mentioned materials were prepared in the 200 μl microtubes and placed in a polymethylmethacrylate (PMMA) phantom (Iran). CT imaging was performed through clinical CT modality (Neusoft) with the parameters of: 1. tube voltages: 90, 120, and 140 kVp, 2. tube current: 250 mA, 3. exposure time: 1000 milliseconds, 5. thickness cutting: 1 mm, 6. Scanning Field of View (SFOV): 250×250 mm, 7. pitch: 1. The attenuation intensity was done in the region of interest (ROI) of the acquired images.

### Cell culture

Human breast cancer cells (MCF-7) were cultured in RPMI 1640 medium (51800-035., GIBCO, USA) with 10% FBS and 1% penicillin-streptomycin (P4333, Sigma Aldrich, USA). The MCF-7 cells were incubated in 37°C, 5% CO<sub>2</sub> for 24 hours.

### Cytotoxicity test

MTT method was used to estimate the cytotoxicity

of Bi2S3 @ BSA-Triptorelin and Bi2S3 @ BSA NPs at concentrations of 0-200 µg/ml ranges. Subsequently, 10<sup>4</sup> MCF-7 cells per well were seeded for 24 hours incubation under 37°C and 5% CO<sub>2</sub>. Then, the each wells medium was replaced with fresh medium of Bi2S3 @ BSA-Triptorelin and Bi2S3 @ BSA with various concentrations from 0-200 µg/ml of nanoparticles. After 24 hours, an appropriate concentration of MTT solution (10 µl of MTT solution per 100 µl) was added to each sample and incubated for 4 hours. Then the medium was removed attentively and added 100 µl of dimethyl sulfoxide (DMSO, D2650, Sigma Aldrich, USA). The absorbance of each well was measured through a microplate absorbance reader (Stat Fax 2300, USA) at 570 nm.

**In vitro CT imaging of MCF-7 cancer cells**

MCF-7 cells were seeded in the 6-well plates with a density of 5×10<sup>5</sup> cells per each well. After that, MCF7 cells were incubated with Bi2S3 @ BSA Triptorelin and Bi2S3 @ BSA NPs at a concentration of 0-75 µg/ml range. The cells were washed 3 times with PBS and then trypsinized. The trypsinized cells were centrifuged and the cell suspension supernatant was removed from the cell plaque. The remaining cells plaque was transferred to 200 µl microtubes and 0.4% agarose gel solution (A9539, Sigma Aldrich, USA) was added on the cell plate to fix the cells. The microtubes were placed in phantom cavities for imaging. The CT values (HU) were caught at the similar workstation through software provided through the manufacturer. The contrast-to-noise ratio (CNR) was obtained using the Hounsfield unit (HU), which is recorded by an analysis that draws a ROI on the chosen image. The CNR was measured as equation (1).

$$\text{Equation (1): } \text{CNR} = (x_s - x_{BG}) / \sigma_{BG}$$

Among them, X<sub>s</sub> and X<sub>BG</sub> are the signal intensities derived in two different structures of interest in the same image. At the same time, σ<sub>BG</sub> is the standard deviation of the background noise in the image. The workflow of this study is illustrated in Figure 1.

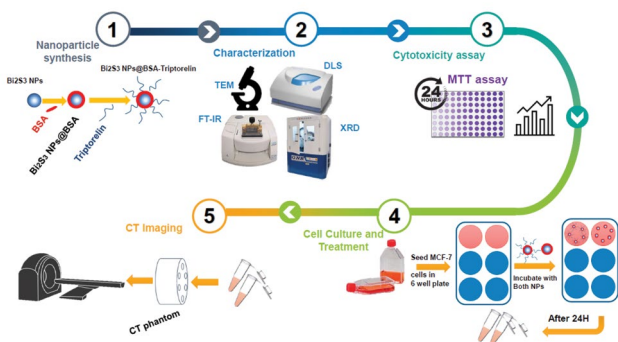


**Fig.1:** Work flow of this study.

**Statistical analysis**

Statistical analysis was done using SPSS software version 22 (IBM, USA). A one-way analysis of variance (ANOVA) was done to evaluate the statistically significant differences between the means of groups and the P<0.05 was assumed statistically significant.

**Results**

**Synthesis and characterization of nanoparticles**

Solutions of Bi2S3 @ BSA and Bi2S3 @ BSA-Triptorelin NPs were synthesized using the protocols described above. The size and morphology of the formed Bi2S3 @ BSA-Triptorelin NPs were determined using TEM (Fig.2).

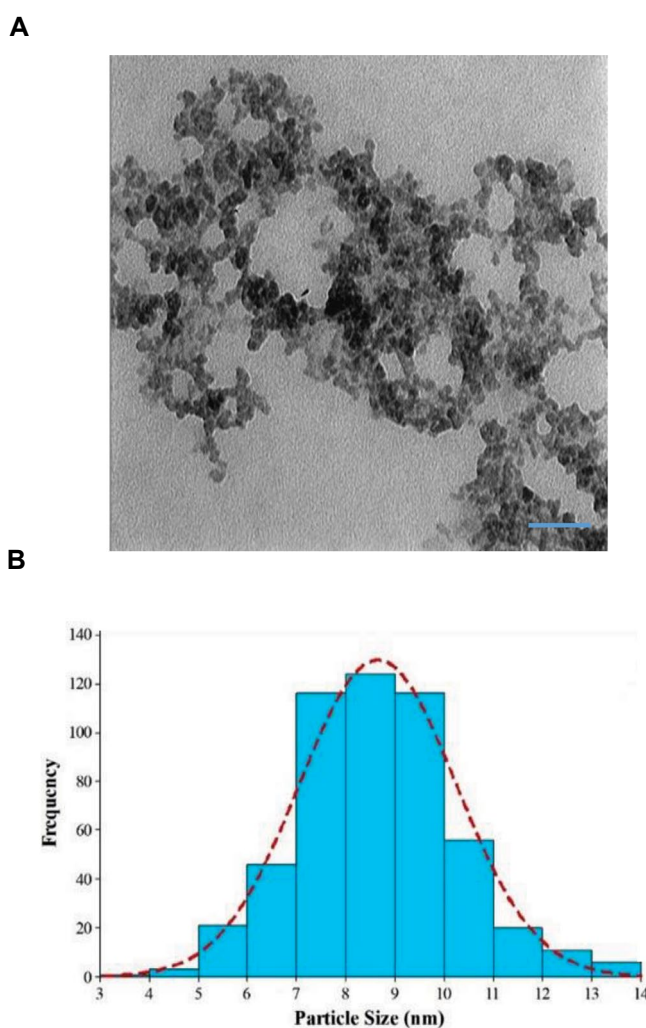


**Fig.2:** Characterization of targeted Bismuth nanoparticles. **A.** Transmission electron microscope (TEM) image (scale bar: 50 nm) and **B.** Size distributions of Bi2S3 @ BSA-Triptorelin NPs. NPs; Nanoparticles.

It may be noted that the formed Bi2S3 @ BSA-Triptorelin NPs have a circular shape with an average size of 8.6 ± 1.6 nm. The hydrodynamic size of Bi2S3 @ BSA and Bi2S3 @ BSA-Triptorelin NPs were measured by DLS at 14.8 nm and 17.1 nm, respectively (Fig.S1A, B, See Supplementary Online Information at www.celljournal.org). Furthermore,

the hydrodynamic size of Bi<sub>2</sub>S<sub>3</sub>@BSA-Triptorelin NPs showed good stability in the culture medium. It was  $17.2 \pm 1.1$  nm after 24 hours incubation (Fig.S1C, See Supplementary Online Information at [www.celljournal.org](http://www.celljournal.org)).

We observed that the surface potential of Bi<sub>2</sub>S<sub>3</sub> @ BSA and Bi<sub>2</sub>S<sub>3</sub> @ BSA-Triptorelin NPs were -77.8 mV and -84.7 mV, respectively (Fig.S2, See Supplementary Online Information at [www.celljournal.org](http://www.celljournal.org)).

The Triptorelin binding to the bismuth sulfide nanoparticles was confirmed by comparing the FTIR spectra of Bi<sub>2</sub>S<sub>3</sub> @ BSA-Triptorelin with Bi<sub>2</sub>S<sub>3</sub> @ BSA NPs. As shown in the Figure 3, the formation of 1651 and 1576 peaks related to the Amide and Primary Amine bonds in the FTIR spectrum of non-peptide bismuth nanoparticles that indicates the BSA presence on the nanoparticles. On the other hand, the removal of the thiol peak of region 2360 is due to the complex formation of bismuth and thiol, which leads to the bismuth bonding with a sulfur that results in a sulfide bond. Also, 670 peak can be related to bismuth sulfide bond. The 3412 peak is related to N-H and O-H stretching vibration. Also, 2921 and 2847 peaks relate to the C-H stretching vibration. The FTIR spectrum of peptide nanoparticles shows that the peptide binds to the nanoparticle surface via an amide bond, which together with BSA-related amides appeared on the nanoparticle surface in 1651 peak. On the other hand, the presence of 702 peak indicates the bond of aromatic C-H, which is related to the aromatic ring of the Triptorelin peptide compound.

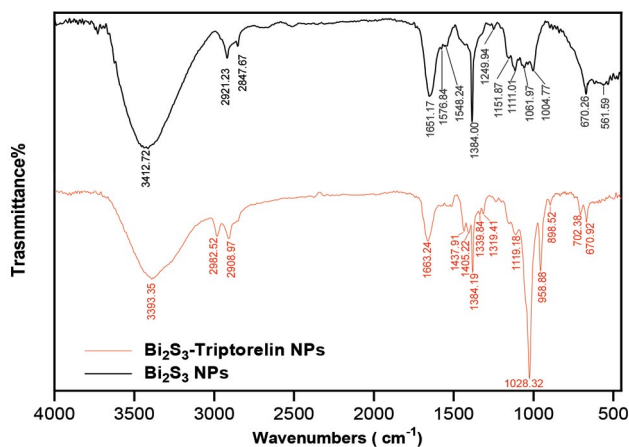


**Fig.3:** FTIR spectra of Bi<sub>2</sub>S<sub>3</sub> @ BSA and Bi<sub>2</sub>S<sub>3</sub> @ BSA-Triptorelin NPs; Nanoparticles.

The crystallographic structure of the synthesized nanoparticles was investigated by the XRD in the range of  $80^{\circ}$ - $20^{\circ}$ . For this purpose, the powder sample was tested. By adapting the diffraction pattern shown in the figure with the reference codes related to the crystal structures of different materials, it can be seen that this pattern is related to the Bi<sub>2</sub>S<sub>3</sub> crystal structure with the reference code JCPDS No. 96-900-3474. The nanoparticles have an Orthorhombic crystal system with lattice constants  $a=11.345$  Å,  $b=3.994$  Å,  $c=11.193$  (Fig.S3, See Supplementary Online Information at [www.celljournal.org](http://www.celljournal.org)).

### X-ray attenuation measurements of Bi<sub>2</sub>S<sub>3</sub>@BSA-Triptorelin nanoparticles versus Visipaque

X-ray attenuation properties of Bi<sub>2</sub>S<sub>3</sub> @ BSA-Triptorelin were compared with an iodine-based small molecule contrast media (Visipaque) as a contrast media concentration function (iodine or bismuth) and X-ray tube potentials difference (Fig.4). As represented in Figure 4, the attenuation intensity of targeted NPs, and Visipaque are increased follow of materials concentration increasing at the different kVp. The X-ray attenuation of targeted nanoparticles versus Visipaque was 3.57 times at 90 kVp and 3000 µg/ml concentration.

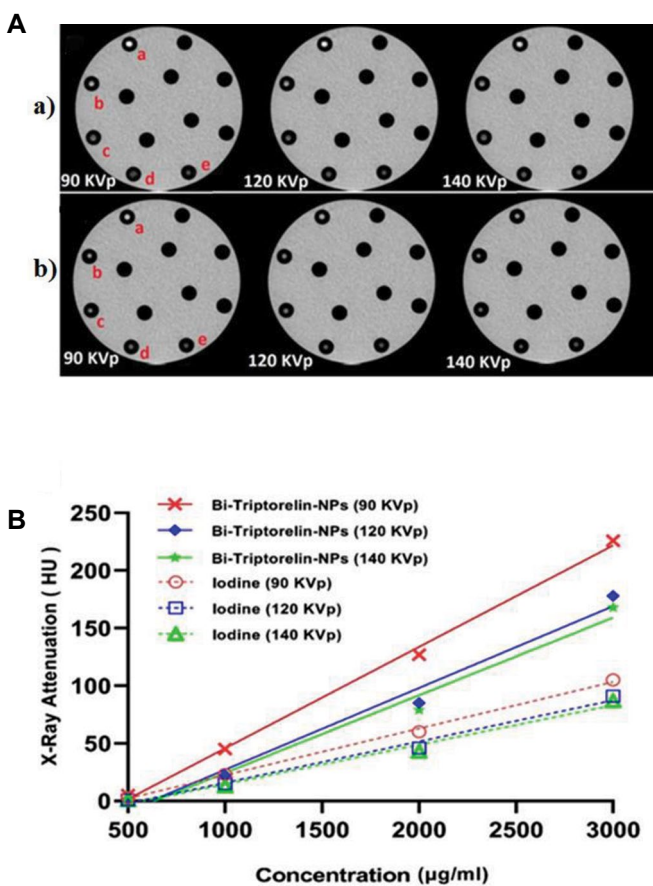


**Fig.4:** CT images and X-ray attenuations intensity of targeted Bismuth NPs and Visipaque at different concentrations and tube potentials. **A.** CT images of Bi<sub>2</sub>S<sub>3</sub> @ BSA-Triptorelin NPs (a) and Visipaque (b) at different concentrations (a; 3000 (µg/ml), b; 2000 (µg/ml), c; 1000 (µg/ml), d; 500 (µg/ml), e; Deionized water) and tube voltages. **B.** Diagram of Attenuation X-ray intensity (HU) of Bi<sub>2</sub>S<sub>3</sub> @ BSA-Triptorelin NPs and Visipaque at different tube potentials and concentrations. CT; Computed Tomography and NPs; Nanoparticles.

### Cytocompatibility assays

We performed the MTT assay to evaluate the toxicity of Bi<sub>2</sub>S<sub>3</sub> @ BSA-Triptorelin and Bi<sub>2</sub>S<sub>3</sub> @ BSA nanoparticles in the MCF-7 cell line. Survival of the cells was measured at two groups of nanoparticles and a wide range of concentrations (0 to 200 µg/ml). The cell survival was decreased with increasing concentration in the both groups of bismuth nanoparticles (Fig. S4, See Supplementary Online Information at [www.celljournal.org](http://www.celljournal.org)). Cytotoxicity was not significant in the

group of peptide-targeted nanoparticles and non-target nanoparticles up to 75 and 150  $\mu\text{g/ml}$ , respectively, compared with the control group ( $P>0.05$ ).

### Targeted CT imaging of MCF-7 cells *in vitro*

In the next step, we investigated the possibility of using Bi2S3 @ BSA-Triptorelin for targeted cells imaging. Figure 5A shows an axial image of CT images of MCF-7 cells with bismuth nanoparticles with and without Triptorelin in different concentrations and kilo voltages (5). As shown in Figure 5B, at 90 kVp and 75  $\mu\text{g/ml}$ , the X-ray attenuation intensity of cells in the presence of targeted nanoparticles is 1.4 times greater than cells in the presence of non-targeted nanoparticles.

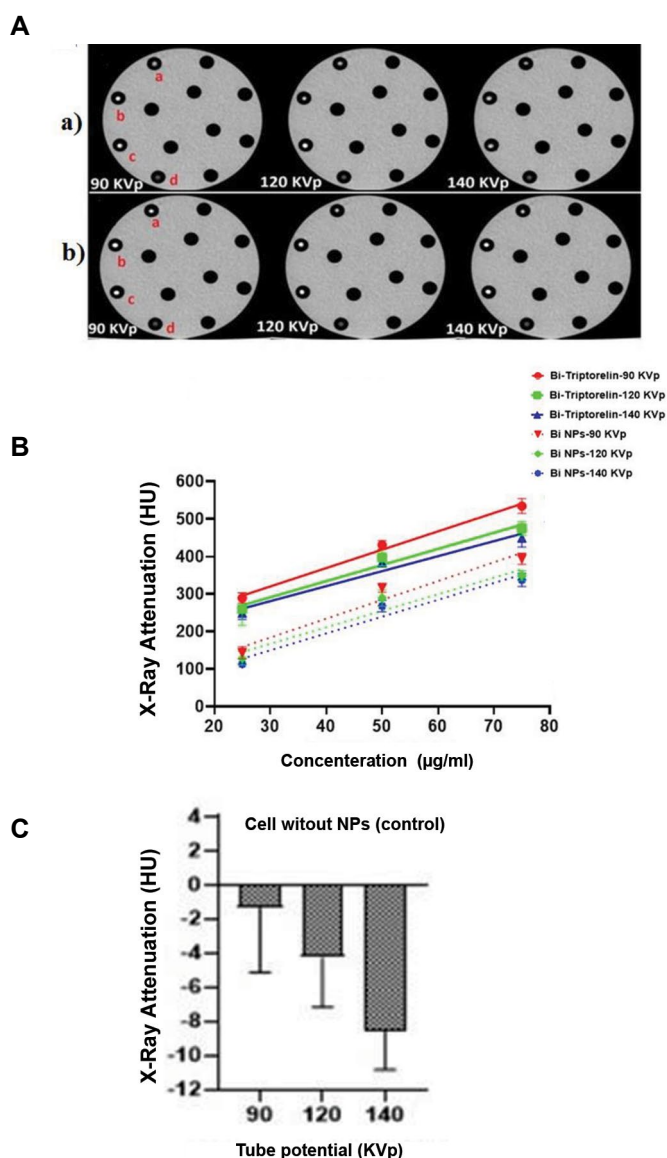


**Fig.5:** CT images and X-ray attenuation intensity of targeted and non-targeted bismuth nanoparticles at different concentrations and X-ray tube potential. **A.** Axial CT images of MCF-7 cells incubated with (a) Bi2S3@BSA and (b) Bi2S3@BSA-Triptorelin NPs at different concentrations [a; 25 ( $\mu\text{g/ml}$ ), b; 50 ( $\mu\text{g/ml}$ ), c; 75 ( $\mu\text{g/ml}$ ), d; MCF-7 cells without presence of NPs]. **B.** Diagram of X-ray Attenuation intensity (HU) of Bi2S3@BSA and Bi2S3 @ BSA-Triptorelin NPs at different tube potentials and concentrations. **C.** Diagram of X-ray attenuation intensity of MCF-7 cells without NPs at different tube potentials. CT; Computed Tomography and NPs; Nanoparticles.

### Investigation of contrast-to-noise ratio of nanoparticle-treated cells

Based on mentioned equation (1), the CNR of cells in the presence of targeted and non-targeted nanoparticles was calculated. The sample without the nanoparticles was considered as the background. At the different voltages, the amount of CNR was obtained according to the amount of attenuation and noise of cell images. The results are summed up in the Figure 6. The results show that the targeted bismuth nanoparticles have greater CNR versus the non-target nanoparticles at the same voltages and concentrations. At 90 kVp and 75  $\mu\text{g/ml}$  concentration, the CNR value showed a 45 unit difference between targeted and non-target nanoparticles. The CNR value was decreased by increasing the tube potential and decreasing the concentration. At 90 kVp and 75  $\mu\text{g/ml}$ , the CNR value of targeted cells is 1.4 times rather than non-targeted cells.

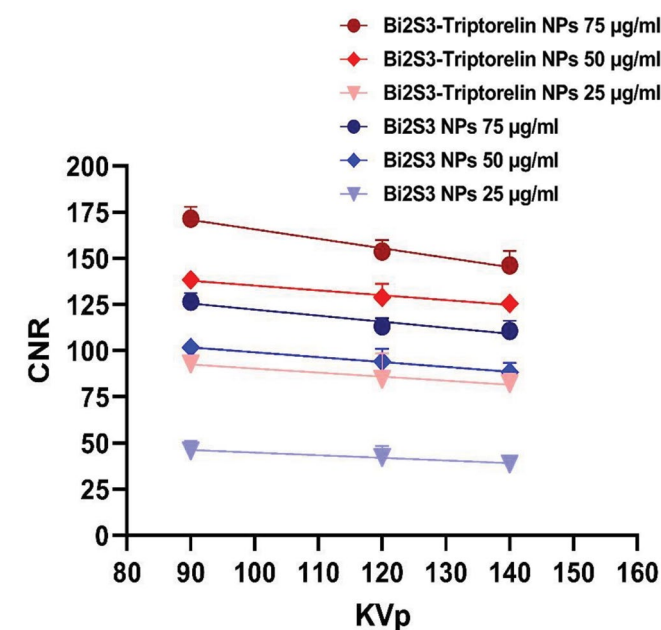


**Fig.6:** CNR obtained from CT images of cancer cells in the presence of targeted and non-targeted NPs. CNR; Contrast to Noise Ratio, CT; Computed Tomography, and NPs; Nanoparticles.

### Discussion

The brightness of CT images and X-ray attenuation intensity were increased with increasing concentration of Bi2S3 @ BSA-Triptorelin NPs and iodine contrast agent. However, the CT values of Bi2S3 @ BSA-Triptorelin NPs was greater than Visipaque with the same concentration. For example, the X-ray attenuation of Bi2S3 @ BSA-Triptorelin was approximately 3.57 times greater than Visipaque at the concentration of 3000  $\mu\text{g/ml}$  and 90 kVp. At 90 keV to 130 keV photon energy range, mass attenuation coefficient of bismuth is higher than Visipaque (22). Bi2S3 @ BSA has a greater attenuation intensity

coefficient than the low molecular weight iodine because of its much greater electron density and atomic number ( $1.69 \times 10^{30}$  e/m<sup>3</sup> and 83) than those of iodine ( $2.34 \times 10^{28}$  e/m<sup>3</sup> and 53), respectively.

We showed that the formed Bi<sub>2</sub>S<sub>3</sub>@ BSA-Triptorelin NPs with a Bi core size of ~8.6 nm are nontoxic in a certain concentration. It should be noted that the employment of Bi<sub>2</sub>S<sub>3</sub>@ BSA-Triptorelin NPs as a contrast medium in a lower concentration and lower side effects has a good potential in the imaging. Ahamed et al. (23) calculated the toxicity of non-targeted Bi<sub>2</sub>O<sub>3</sub> nanoparticles in the MCF-7 cell line. They showed a significant cytotoxicity at the 50 µg/ml concentration. However, at the concentrations above 50 µg/ml, their results indicated more cytotoxicity than our study. Dong et al. (24) evaluated the cytotoxicity of Bi<sub>2</sub>S<sub>3</sub>@ BSA-FA nanoparticles at the concentration of 400 µg/ml on 4T1 cell line. Their results did not show any significant cytotoxicity. In our study, the cytotoxicity of Bi<sub>2</sub>S<sub>3</sub>@ BSA-Triptorelin and Bi<sub>2</sub>S<sub>3</sub>@ BSA NPs was not significant, up to 75 µg/ml and 150 µg/ml, respectively.

Based on several studies, the cytotoxicity of nanoparticles depends on many factors such as cell line type, nanoparticle type, coating, target agents of nanoparticles, and incubation time. Obviously, based on X-ray attenuation intensity, greater concentration leads to greater cellular uptake of both NPs. The CT values of targeted and non-targeted NPs in the MCF-7 cells were much higher than untreated control cells and there was a good statistically significant difference. The highest amount of HU value was related to the targeted bismuth nanoparticles at 90 kVp X-ray tube potential and the concentration of 75 µg/ml. At the same concentration and X-ray tube potential, the HU value of targeted nanoparticles was 1.4 and 398 times greater than the HU value of non-targeted bismuth nanoparticles and the cells without the presence of nanoparticles (control), respectively. Higher CT values of Bi<sub>2</sub>S<sub>3</sub>@ BSA-Triptorelin compared to Bi<sub>2</sub>S<sub>3</sub>@ BSA can be attributed to the targeting of nanoparticles by the Triptorelin peptide and their greater cell uptake via enhancement of internalization of Bi<sub>2</sub>S<sub>3</sub>@ BSA-Triptorelin NPs through GnRH receptors in the MCF-7 cells. In the X-ray imaging, this is hard to visually distinguish the brightness of cancer cells incubated with various concentrations of nanoparticles.

New CTs have a strength of 4096 tons of gray, which produces various densities in HU. But, the human eye cannot detect higher than 20 tons of gray in a CT image. Thus, a CT value is a smaller value representing the actual attenuation of an object's X-rays (HU), which is safer, more specific, and more accurate than an image. The CNR value or CT contrast enhancement of Bi<sub>2</sub>S<sub>3</sub>@ BSA-Triptorelin was significantly higher than cells treated with non-target nanoparticles at the same concentration and tube potential. The results of CT contrast enhancement were related to the X-ray CT attenuation of the contrast media. The CNR value increased by increasing the concentrations of Bi, because of more atoms are existed for interaction at higher concentrations. The CNR value of

Bi<sub>2</sub>S<sub>3</sub>@ BSA-Triptorelin and Bi<sub>2</sub>S<sub>3</sub>@ BSA NPs were decreased by increasing X-ray tube potential range from 90 to 140 kVp. It was in agreement with Algethami et al. (25) study. Our findings propose that Bi<sub>2</sub>S<sub>3</sub>@ BSA-Triptorelin can be targeted MCF-7 cells for particular X-ray imaging utilizations.

## Conclusion

We have provided an easy way to synthesize Bi<sub>2</sub>S<sub>3</sub>@ BSA-Triptorelin for the targeted CT imaging. Our results indicated targeted NPs have a greater X-ray attenuation than non-targeted cells at the same concentration. Furthermore, targeted and non-targeted cells have a higher attenuation intensity rather than iodine contrast media (Visipaque). Our findings revealed that the attenuation intensity and CNR highly depend on the bismuth concentration and the tube potentials. Our findings indicated the Bi<sub>2</sub>S<sub>3</sub>@ BSA-Triptorelin NPs can be applied as a contrast agent for molecular CT of breast cancer. In the future studies, the targeted NPs can be assessed in radiotherapy and *in vivo* study.

## Acknowledgments

The authors gratefully acknowledge the Medical Physics Research Center, Mashhad University of Medical Sciences, Mashhad, Iran. This study was supported by a grant (No: 980650) from Mashhad University of Medical Sciences, Mashhad, Iran. The authors declare that they have no conflicts of interest in this study.

## Authors' Contribution

A.M., S.Kh., M.K.; Contributed to conception and design. M.M., Y.Ch.; Contributed to all experimental work, data and statistical analysis, and interpretation of data. R.I.; Contributed to the synthesis of nanoparticles and interpretation of characterization nanoparticles data. A.M.; Drafted the manuscript. M.K., A.M.; Revised the manuscript. All authors read and approved the final manuscript.

## References

- MacRitchie N, Frleta-Gilchrist M, Sugiyama A, Lawton T, McInnes IB, Maffia P. Molecular imaging of inflammation-Current and emerging technologies for diagnosis and treatment. *Pharmacol Ther.* 2020; 211: 107550.
- Cole LE, Ross RD, Tilley JM, Vargo-Gogola T, Roeder RK. Gold nanoparticles as contrast agents in x-ray imaging and computed tomography. *Nanomedicine.* 2015; 10(2): 321-341.
- Goldman W. Principles of CT: radiation dose and image quality. *J Nucl Med Technol.* 2007; 35(4): 213-225.
- Khademi S, Sarkar S, Shakeri-Zadeh A, Attaran N, Kharrazi S, Ay MR, et al. Folic acid-cysteamine modified gold nanoparticle as a nanoprobe for targeted computed tomography imaging of cancer cells. *Mater Sci Eng C Mater Biol Appl.* 2018; 89: 182-193.
- Zhou D, Li C, He M, Ma M, Li P, Gong Y, et al. Folate-targeted perfluorohexane nanoparticles carrying bismuth sulfide for use in US/CT dual-mode imaging and synergistic high-intensity focused ultrasound ablation of cervical cancer. *J Mater Chem B.* 2016; 4(23): 4164-4181.
- Zhu HL, Cheng QY, Liao MY, Zhang ZL, Cai WG, Ma JJ, et al. Economical synthesis of ultra-small Bi<sub>2</sub>S<sub>3</sub> nanoparticles for high-sensitive CT imaging. *Mater Res Express.* 2019; 6(9): 095005.
- Koç MM, Aslan N, Kao AP, Barber AH. Evaluation of X-ray tomog-

- raphy contrast agents: a review of production, protocols, and biological applications. *Microsc Res Tech*. 2019; 82(6): 812-848.
8. Zheng X, Shi J, Bu Y, Tian G, Zhang X, Yin W, et al. Silica-coated bismuth sulfide nanorods as multimodal contrast agents for a non-invasive visualization of the gastrointestinal tract. *Nanoscale*. 2015; 7(29): 12581-12591.
  9. Luo S, Zhang E, Su Y, Cheng T, Shi C. A review of NIR dyes in cancer targeting and imaging. *Biomaterials*. 2011; 32(29): 7127-7138.
  10. Chen ZY, Wang YX, Lin Y, Zhang JS, Yang F, Zhou QL, et al. Advance of molecular imaging technology and targeted imaging agent in imaging and therapy. *Biomed Res Int*. 2014; 2014: 819324.
  11. James ML, Gambhir SS. A molecular imaging primer: modalities, imaging agents, and applications. *Physiol Rev*. 2012; 92(2): 897-965.
  12. Huerta-Reyes M, Maya-Núñez G, Pérez-Solis MA, López-Muñoz E, Guillén N, Olivo-Marin JC, et al. Treatment of breast cancer with gonadotropin-releasing hormone analogs. *Front Oncol*. 2019; 9: 943.
  13. Deng X, Qiu Q, Ma K, Huang W, Qian H. Synthesis and in vitro anti-cancer evaluation of luteinizing hormone-releasing hormone-conjugated peptide. *Amino Acids*. 2015; 47(11): 2359-2366.
  14. Schally AV, Engel JB, Emons G, Block NL, Pinski J. Use of analogs of peptide hormones conjugated to cytotoxic radicals for chemotherapy targeted to receptors on tumors. *Curr Drug Deliv*. 2011; 8(1): 11-25.
  15. Schally AV, Comaru-Schally AM, Nagy A, Kovacs M, Szepeshazi K, Plonowski A, et al. Hypothalamic hormones and cancer. *Front Neuroendocrinol*. 2001; 22(4): 248-291.
  16. Schally AV, Nagy A. Chemotherapy targeted to cancers through tumoral hormone receptors. *Trends Endocrinol Metab*. 2004; 15(7): 300-310.
  17. Roy J, Kaake M, Low PS. Small molecule targeted NIR dye conjugate for imaging LHRH receptor positive cancers. *Oncotarget*. 2019; 10(2): 152.
  18. Venturelli M, Guaitoli G, Omarini C, Moschetti L. Spotlight on triptorelin in the treatment of premenopausal women with early-stage breast cancer. *Breast Cancer (Dove Med Press)*. 2018; 10: 39-49.
  19. Mező G, Manea M. Receptor-mediated tumor targeting based on peptide hormones. *Expert Opin Drug Deliv*. 2010; 7(1): 79-96.
  20. Zu Y, Yong Y, Zhang X, Yu J, Dong X, Yin W, et al. Protein-directed synthesis of Bi<sub>2</sub>S<sub>3</sub> nanoparticles as an efficient contrast agent for visualizing the gastrointestinal tract. *RSC Adv*. 2017; 7(28): 17505-17513.
  21. Vattikuti SVP, Police AKR, Shim J, Byon C. Sacrificial-template-free synthesis of core-shell C@Bi<sub>2</sub>S<sub>3</sub> heterostructures for efficient supercapacitor and H<sub>2</sub> production applications. *Sci Rep*. 2018; 8: 4194.
  22. De La Vega JC, Häfeli UO. Utilization of nanoparticles as X-ray contrast agents for diagnostic imaging applications. *Contrast Media Mol Imaging*. 2015; 10(2): 81-95.
  23. Ahamed M, Akhtar MJ, Khan MM, Alrokayan SA, Alhadlaq HA. Oxidative stress mediated cytotoxicity and apoptosis response of bismuth oxide (Bi<sub>2</sub>O<sub>3</sub>) nanoparticles in human breast cancer (MCF-7) cells. *Chemosphere*. 2019; 216: 823-831.
  24. Dong L, Zhang P, Liu X, Deng R, Du K, Feng J, et al. Renal clearable Bi-Bi<sub>2</sub>S<sub>3</sub> heterostructure nanoparticles for targeting cancer theranostics. *ACS Appl Mater Interfaces*. 2019; 11(8): 7774-7781.
  25. Algethami M, Blencowe A, Feltis B, Geso M. Bismuth sulfide nanoparticles as a complement to traditional iodinated contrast agents at various x-ray computed tomography tube potentials. *J Nanomater Mol Nanotechnol*. 2017; 9: 25-28.